

# The Role of Nickel Ferrite Magnetic Nanoparticles in Medical Science

Varsha Unni P. K.<sup>1</sup>, Sumilha .M<sup>2</sup>, Roshni .A<sup>3</sup>

**Abstract:** *The nanotechnology industry is accelerating day by day with its inspiring outcomes. These outcomes grease the wheels for smartening our world. This nanotechnology has immense range of applications in the field of aerospace engineering, nano-electronics, environmental remediation and medical healthcare. Nanoparticles are materials having overall size of less than 100 nanometers. These materials have become the key players in modern medicine in recent years, with therapeutic applications ranging from contrast agents in imaging to medication and gene delivery carriers into malignancies. In some cases, nanoparticles make it possible to perform investigations and treatments which would otherwise be impossible. Nanoparticles, on the other hand, provide significant environmental and societal challenges, notably in terms of toxicity. This paper review will focus on nanoparticles major contributions to modern medicine, as well as their environmental and societal implications. In these fields, nickel ferrite nanoparticles play a very advantageous role when compared to other nanoparticles due to its typical physical, chemical and magnetic properties like high electrochemical stability, low conductivity and thus negligible eddy current loss, abundance in nature and the most important property of ferrite nanoparticles is the reduction in saturation magnetization ( $M_s$ ) related to the bulk ferrite counterpart. The decrease in ( $M_s$ ) is linked to ins and outs, such as surface effects. This paper reviews mainly focuses on the structural behavior, magnetic properties, synthesis methods and concludes with some of its medical applications which includes hyperthermia, magnetic resonance imaging (MRI), magnetic separation and drug delivery of nickel ferrite nanoparticles.*

**Keywords:** Nickel ferrite, Cation distribution, Biomedicine, Saturation magnetization, Coprecipitation

## 1. Introduction

Ferrite is a significant material having both electrical and magnetic properties which is formed by heating iron oxides and it is combined with small proportions of one or more additional elements such as Nickel, Zinc and Magnesium. In twelfth century, the ancient Chinese were known to utilize lodestone ( $Fe_3O_4$ ) in a mariner's compass for route [1]. The naturally occurring magnetite with the chemical formula  $Fe_3O_4$  is a weak hard ferrite. Hard ferrites have magnetism which is basically a permanent material having high coercive field. Other kinds of ferrite are called soft ferrites which are not difficult to magnetize and demagnetize and have low coercive field. The magnetic materials with low coercivity of the order of 12.5 Oersted are named as soft and those with coercivity above the order of 12.5 Oersted are hard magnetic materials [2].

The molecular formula of ferrites is  $M^{2+}OFe_2^{3+}O_3$ , where M represents the divalent metal like Fe, Mn, Cu, Co, Zn, Ni, Mg and much more. The soft ferrites properties are of saturation magnetization, initial permeability, magnetic loss factor, remanence, coercive force, Curie temperature, resistivity, dielectric constant, thermopower and so forth.

In the year 1909, S. Hilpert published magnetization curves as a function of temperature for nickel, magnesium, copper and zinc ferrites [3]. Since 1909, when S. Hilpert reported his study on magnetic insulator, many specialists have dealt with ferrites to discover new ferrites with specific electrical and magnetic properties. The two components which are responsible for the electrical and magnetic properties of prepared ferrites are sintering conditions and the method of preparation. Among the different types of ferrites, as specifically spinel ferrites are widely used in electrical and

magnetic applications [4], [5]. In 1915, Bragg and Nishikawa determined the spinel structure in ferrites [6],[7].

**Nickel ferrite:** The nickel ferrite ( $NiFe_2O_4$ ) is a well-known spinel magnetic material and which is prepared by solid state reactions in which the solid reactants are heated to produce a new solid composition, high temperature is required for sintering and aggregation of particles [8]. Because of its fundamental properties, the researchers continued their efforts on ferrites especially nickel ferrite in the medical applications. Nickel ferrite possess appealing properties such as low Curie temperature as the particle size decreases, high electrical resistivity and consequently low eddy current losses which make them suitable in the field of medicine and healthcare treatment over biocompatibility and low toxicity [9]. **Table 1** represents the main magnetic parameters ( $M_s, M_R, H_C, K$ ), particle diameter, and synthesis method for nickel ferrite [10]. To produce magnetic nanoparticles of nickel ferrite mostly prepared by sol-gel method and co-precipitation techniques. In these two techniques has its own pros and cons. For example; when nickel ferrite synthesized by sol-gel method had bigger crystalline structure whereas in the co-precipitation method they are irregular in shape and saturation magnetization increases with increasing the annealing temperature in both the techniques. The application of nickel ferrite such as fabrication of ferrofluids, catalysis, gas sensors, magnetic liposomes [11], magnetic polymeric nanoparticles, MRI, hyperthermia treatment especially for magnetically guided drug delivery system [12], biosensor (cholesterol biosensor). Furthermore, they are characterized by means of powder x-ray diffraction, scanning electron microscopy, Transmission electron microscopy and Fourier transform infrared Spectroscopy. **Fig 1** shows the properties, synthesis methods and applications of nickel ferrite.

**Table 1:** Average crystalline size (D), saturation magnetization ( $M_S$ ), remanent magnetization ( $M_R$ ), coercivity ( $H_C$ ) and anisotropy constant (K) of  $NiFe_2O_4$

Synthesis method	Temp.	$D_{XRD}(nm)$	$M_S[emu/g]$	$M_R[emu/g]$	$H_C[kOe]$	$K*10^3[erg/cm^3]$	Ref.
Sol-gel	RT	23.0	20.1	6.82	0.061	0.770	[13]
Sol-gel	RT	70.0	37.3	—	0.321	—	[14]
Sol-gel auto-combustion	RT	58.0	50.0	7.00	0.050	—	[15]
o-precipitation	RT	17.3	43.9	16.6	0.051	—	[16]
combustion	RT	25.0	30.2	4.00	0.159	—	[17]
Microwave combustion	RT	18.5	37.9	2.57	0.016	—	[18]
hydrothermal	RT	8.20	31.9	—	0.007	—	[19]
Thermal decomposition	RT	25.0	36.5	10.6	0.263	—	[20]
Thermal decomposition	RT	79.0	43.60	17.63	0.645	—	[21]
Thermal decomposition	RT	10.7	36.8	—	—	—	[22]

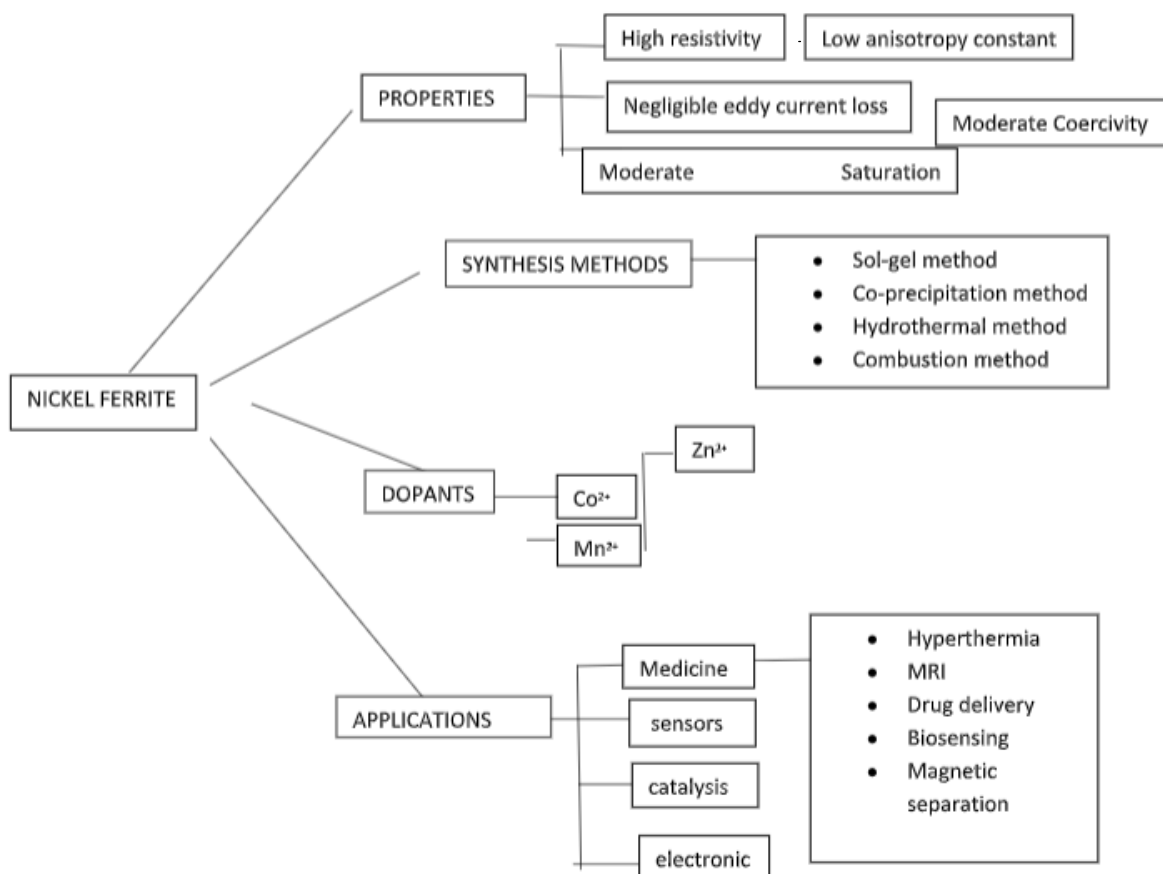


**Figure 1:** Properties, synthesis method and applications of nickel ferrite

**Crystal Structure of Nickel ferrite:** Nickel ferrite has an inverse spinel structure with a general formula  $(B(AB)O_4)$ , where [A] is the divalent ion and [B] is the trivalent ion. Nickel ferrites are soft material with no preferred direction of magnetization. It is relatively easy to change the direction by applying external magnetic field. Due to its significant magnetic behaviors, it is further investigated. From the crystallography viewpoint, the inverse spinel structure of nickel ferrite with  $Ni^{2+}$  ions on octahedral i.e., [B]- sites denoted Oh sites and  $Fe^{3+}$  ions will occur between tetrahedral i.e. [A]- site ions denoted as Td sites and octahedral sites, furthermore oxygen atom is added in order to complete the cubic crystal structure. Thus, an inverse spinel can be represented as:  $(Fe^{3+}(Ni^{2+}Fe^{3+})O_4^{2-})$ [23],[24]. In the case of nickel ferrite inverse spinel, the crystal field stabilization energy (CFSE) is comparatively greater in divalent ion  $[A^{2+}]$  than the trivalent ion  $[B^{3+}]$  in octahedral geometry. Hence, they show ferrimagnetism. According to super exchange interaction (B-O-B) i.e.,  $(Fe^{3+}-O-$

$Fe^{3+})$  magnetic interaction is possible between metal ions and through the intermediate oxygen ions. The cation distribution of B-B sites of the spinel depends on the bond length and bond angle. The inverse spinel structure of  $NiFe_2O_4$  is constructed by filling the face-centered cubic (FCC) lattice points were shown in **Figure 2**[25]. The different values of the inter-atomic distances for  $NiFe_2O_4$  are listed in **Table 2**. Also, **Table 3** represents the variation of different inter-ionic distances as a function of the synthesis methods for nanocrystalline  $NiFe_2O_4$  (Å). The magnetic properties such as saturation magnetization and Curie point are affected by this variation in their inter-ionic distances.

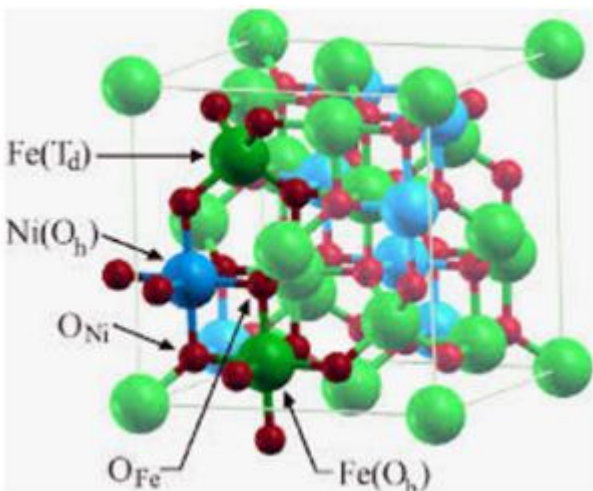


Figure 2: Schematic representation of inverse nickel ferrite structure

Table 2: The inter-atomic distances between the cations on the tetrahedral (A) and octahedral (B) sites are given below [26].

$R_A-R_A$	$R_A-R_B$	$R_B-R_B$	$R_A-O_A$	$R_B-O_B$
$(\frac{\sqrt{3}}{4})a$	$(\frac{\sqrt{\pi}}{4})a$	$(\frac{\sqrt{2}}{4})a$	$a\sqrt{3}(\delta + \frac{1}{8})$	$a\sqrt{3}[\frac{1}{16} - \frac{\delta}{2} + 3\delta^2]^{\frac{1}{2}}$

$\delta$ : is the deviation from oxygen parameter (U),  $\delta=U-U_{ideal}$ .  $R_A$  and  $R_B$ : which refer to the cations at the center of the tetrahedral [A] and octahedral [B] sites, respectively,  $O_A$  and  $O_B$ : the center of oxygen anions that is related to the tetrahedral [A] and octahedral [B] configurations, where a is the lattice parameter respectively.

Table 3: Calculated values of inter atomic distances for nanocrystalline  $NiFe_2O_4$  (Å) are given below.

Method	Composition	X	$R_A-R_A$	$R_A-R_B$	$R_B-R_B$	$R_A-O_A$	$R_B-O_B$	Ref.
Co-precipitation	$NiFe_2O_4$	0.93	3.6091	3.6933	2.9468	1.8733	2.0435	[27]
Sol gel	$NiFe_2O_4$	1.6	3.092	3.6529	2.915	1.785	2.0615	[28]
		0.8	3.088	3.6485	2.912	1.783	2.059	
		0.6	3.085	3.6450	2.909	1.781	2.057	
		0.4	3.090	3.6503	2.913	1.784	2.060	

**Dopants:** Doping is the method of adding foreign elements. It can modify the chemical and magnetic properties, specifically the application of nickel ferrite is enhanced with the doping of various oxides. For nickel, the most important oxides are  $Zn^{2+}$ ,  $Co^{2+}$  and  $Mn^{2+}$  will be discussed in detail.

**$Zn^{2+}$  ion:** Nanocrystalline powders of  $Ni_{1-x}Zn_xFe_2O_4$  ( $x = 0.0, 0.2, 0.4, 0.6, 0.8$ ) have been prepared through utilizing an oxalic-acid-based precursor technique. The particle size was found to decrease as the composition of Zn content is increased. The Zn ions have greater ionic radii when compared to Ni ions, the lattice constants were found to increase with increasing Zn content. Due to the uncoupled spins and weakening of the A-B interactions, the magnetization is increased up to  $x = 0.4$  and then decreased. With increased Zn concentration, the coercivity was shown to decrease. This could be because there is a change in the anisotropy energy density (K) and in the volume (v) of nanoparticles. The modification of magnetic properties such as coercivity and saturation magnetization were shown in Table 3 [29].

Table 3: Particle size D, lattice parameter values a, coercivity  $H_c$ , remanence magnetization  $M_r$  and maximum magnetization at M for nanocrystalline  $Ni_{1-x}Zn_xFe_2O_4$  ( $0.0 \leq x \leq 0.8$ ) nanoparticles.

x	D [nm]	a [Å]	$H_c$ [Oe]	$M_r$ [emu/g]	M [emu/g]
0.0	26	8.285	144	8.52	34.6
0.2	23	8.311	139	14.8	57.4
0.4	22	8.355	106	11.9	63.1
0.6	19	8.415	55	6.6	52.7
0.8	17	8.423	22	1.4	24.3

**$Co^{2+}$  ion:** With the general formula  $Ni_{1-x}Co_xFe_2O_4$  having ( $x=0.0, 0.1, 0.2, 0.3, 0.4$ ) nanoparticles are synthesized effectively by heat treatment process. The XRD data showed

that when the addition of  $Co^{2+}$  content increases, the lattice constant and volume of the unit cell are increased while X-ray density decreases. The Field Emission Scanning Electron Microscope (FESEM) micrograph shows the irregular morphology of the prepared  $Ni_{1-x}Co_xFe_2O_4$  nanoparticles. The  $Ni_{1-x}Co_xFe_2O_4$  nanoparticles were formed at  $600^\circ C$ , according to Thermo-gravimetric analysis (TGA). The Mossbauer spectroscopic graph revealed an extra sextet line for  $x=0.4$  with regard to  $x=0.0$ , this is because of the presence of unreacted Fe. The M-H curve analysis discovered that the coercivity increases with increasing  $Co^{2+}$  concentration, with the maximum value of coercivity (1608 Oe) found for ( $x=0.4$ ), which could be related to the presence of unreacted Fe. As a result,  $Ni_{1-x}Co_xFe_2O_4$  ( $x=0.4$ ) can be employed in magnetic applications as a magnetic material.

Table 4: Room temperature measurement of coercivity ( $H_c$ ), remanent magnetization ( $M_r$ ), and saturation magnetization (M) of  $Ni_{1-x}Co_xFe_2O_4$  (0.0, 0.1, 0.2, 0.3, 0.4) samples [30]

x	D [nm]	a [Å]	$H_c$ [Oe]		$M_r$ [emu/g]		M [emu/g]	
			RT	2.5K	RT	2.5K	RT	2.5k
0.0	25	8.3157	263	270	10.60	7.50	36.54	43.74
0.1	27	8.3319	572	-	11.19	-	32.07	-
0.2	28	8.3389	995	3530	16.27	37.77	37.93	49.43
0.3	29	8.3432	1204	-	16.53	-	32.40	-
0.4	31	8.3432	1608	8430	20.99	38.27	43.25	47.63

**$Mn^{2+}$  ion:** Manganese substituted nickel ferrite nanoparticles of chemical composition  $Ni_{1-x}Mn_xFe_2O_4$  samples ( $x = 0, 0.2, 0.4, 0.6$ ) were synthesized at room temperature by a sol-gel auto combustion technique.  $Ni_{1-x}Mn_xFe_2O_4$  has a cubic spinel structure which was shown by XRD pattern. The Mn substituted Ni ferrite nanoparticles were found to be superparamagnetic at room temperature, according to the

VSM analysis. The coercivity and remanent magnetization values are decreased. With the increasing concentration of  $Mn^{2+}$  ion, the g value decreases. The surface morphology investigated that the ferrite samples are spherically shaped and the size were found to be from 22 to 41nm. In **Figure 3**, FTIR spectrum represents the two main metal-oxygen vibrations that are seen at  $550$  to  $560\text{ cm}^{-1}$  and at  $449$  to  $480\text{ cm}^{-1}$  which is due to tetrahedral and octahedral sites, respectively[31]. It is presumed that substituted manganese ion firmly influences the magnetic and structural properties of nickel ferrite. The magnetic properties and EPR parameters (g value) of  $Ni_{1-x}Mn_xFe_2O_4$  were shown in **Table 5**[31].

**Table 5:** Magnetic properties of the Mn-substituted Ni ferrite samples and the EPR parameters

x	a [Å]	$H_c [O_e]$	$M_r$ [emu/g]	Resonance field, $H_r$ [G]	g value
0	8.355	200	0.100	-	-
0.2	8.473	110	0.075	2250	3.131
0.4	8.439	70	0.050	2500	2.817
0.6	8.451	60	0.025	3050	2.012

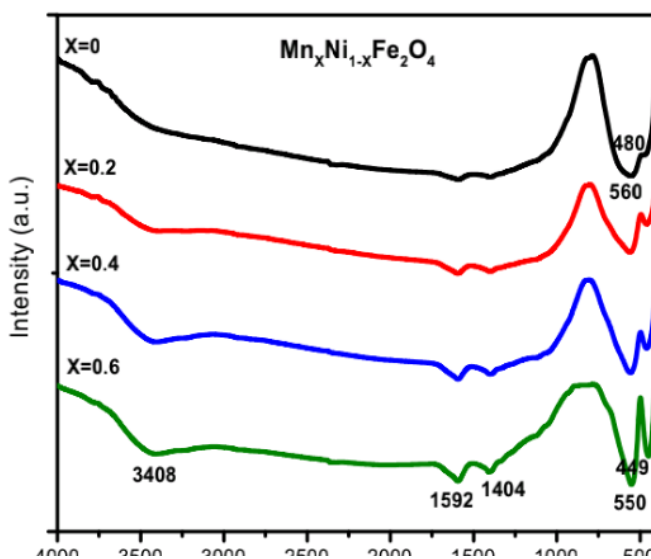


**Figure 3:** FTIR spectrum of the  $Ni_{1-x}Mn_xFe_2O_4$  samples ( $x = 0, 0.2, 0.4, 0.6$ ).

**Synthesis Methods:** The impact of synthesis method can affect the cation distribution, particle size and size distributions and subsequently the magnetic properties and applications of nickel ferrite nanoparticles particularly in medical science. To examine the size dependent structural and magnetic behavior, various methods used to synthesize the nanoparticles such as sol - gel method, co-precipitation, reverse micelle method and so on. Because of its low-cost precursors and quick reaction time, co-precipitation may be the most promising of the many approaches. It is generally utilized for biomedical applications because of its simplicity, economic and reproducibility. The cation distribution of the nanoparticles relies on the parameters, such as the cation radii, particle size and it is determined from synchrotron powder diffraction data using synchrotron radiation. The cation distribution on A-site and B-site for nanosized nickel ferrite prepared sample for different synthesis method is given in **Table 6**. The magnetic properties of ferrites were explained by Neel [32], who proposed that the magnetic

moments of ferrites are the sum of magnetic moments of individual sublattice  $M_A$  and  $M_B$ . The magnetic moments of ferrites in the A and B sites are antiparallel, whereas those in the B-sites are parallel to each other. For nickel ferrite the magnetic ions and their magnetic moment are  $Ni^{2+} = 2\mu_B$  and  $Fe^{3+} = 5\mu_B$  respectively [33],[1]. Magnetic moments for nanocrystalline  $NiFe_2O_4$  were tabulated in **Table 7**.

**Table 6:** Cation distribution on A site and B site for  $NiFe_2O_4$

Method of synthesis	Composition (x)	Cation distribution (A site)	Cation distribution (B site)	Ref.
Sol gel	1.6	$(Ni_{0.6}Fe_{1.6})$	$[Ni_{1.6}Fe_{1.6}]$	[28]
	0.8	$(Ni_{0.2}Fe_{0.8})$	$[Ni_{0.8}Fe_{1.2}]$	
	0.6	$(Ni_{0.4}Fe_{0.6})$	$[Ni_{0.6}Fe_{1.4}]$	
	0.4	$(Ni_{0.6}Fe_{0.4})$	$[Ni_{0.4}Fe_{1.6}]$	
Spray Pyrolysis	0.89	$(Ni_{0.11}Fe_{0.89})$	$[Ni_{0.89}Fe_{1.11}]$	[34]
Co-precipitation	0.93	$(Ni_{0.07}Fe_{0.93})$	$[Ni_{0.93}Fe_{1.07}]$	[27]

**Table 7:** Calculated values for magnetic moment for nanocrystalline  $NiFe_2O_4$

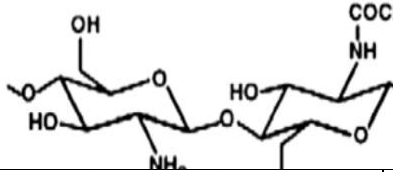
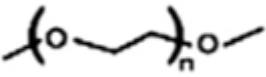
Method of synthesis	Composition (x)	$M_A$ ( $\mu_B$ )	$M_B$ ( $\mu_B$ )	$\mu$ (/molecule)	Ref.
Co precipitation	$NiFe_2O_4$	4.79	7.21	2.42	[27]
combustion method	$NiFe_2O_4$	2	5	3	[35]
Spray Pyrolysis	$NiFe_2O_4$	-	-	1.77	[34]

where,  $M_A$  and  $M_B$  representing the magnetic moments of A - site (tetrahedral) and B- site (octahedral) respectively.

**Some Compatible Coatings:** The surface coatings of nanoparticles are frequently applied in one or more layers in determining the magnetic nanoparticles for specific application. Significantly, the coating material should be in the form of ferrofluids. Without a coating, the magnetic nanoparticles have hydrophobic surfaces with large surface area to volume ratios and behave in a particular way to agglomerate. Surface coatings eliminates the adverse effects of nanoparticles. Furthermore, a proper surface coating material improves the stability and saturation magnetization of the magnetic nanoparticles. Various kinds of coating materials are used to modify the magnetic behavior of nanoparticles they are organic polymers, organic surfactants, inorganic metals, inorganic oxides, bioactive molecules, (modifies the surface charge or composition) it is analyzed by FTIR absorption spectrum. Since the magnetic nanoparticles are toxic, surface modification is required in order to apply them to the human body. It is also required for labelling the chemicals such as drugs and targeting ligands onto the surfaces. The biocompatible material called Poly ethylene glycol (PEG) is coated to nickel ferrite nanoparticles consequently, a rod-shaped nickel ferrite nanoparticle was prepared for magnetic hyperthermia in cancer treatments. Also, Chitosan coated nickel ferrite nanoparticles were used as contrast agent in MRI and as drug delivery carriers to the target in the treatment of cancer cells. [36].



**Table 8:** Properties of natural and synthetic polymers for coating magnetic nanoparticles

Polymer	Structure	Biocompatibility	Hydrophobicity	Applications	Ref.
Natural polymers: Chitosan		Biocompatible Nontoxic	Hydrophilic	Drug delivery MRI Hyperthermia	[37],[38]
Synthetic polymers: Poly (ethylene glycol) (PEG)		Biocompatible	Hydrophilic	Drug delivery MRI Hyperthermia	[39]-[43]

**Medical Applications:** The use of magnetic nanoparticles became the prominent one because of its interesting characteristics for introducing novel synthesis techniques, applications especially in the medical treatment. Moreover MRI, drug delivery, hyperthermia and biosensors are the promising ones in the biomedical application.

**Hyperthermia:** Well-dispersed nickel ferrite nanoparticles give effective and controlled heat generation in the cancer hyperthermia application. Nickel ferrite nanoparticles with moderate saturation magnetization and sizes lying within the superparamagnetic ferrimagnetic transition region are suitable for the hyperthermia application. The amount of heat that nickel ferrite nanoparticles generate can be determined by the magnetic moment, field, frequency because the heat generation is described by power loss due to Neel and Brownian relaxation mechanisms. By the theoretical description, the power loss is given by:

$$SAR = \frac{P}{\rho} = \frac{\mu_0 \pi}{\rho} f H_0^2 \chi'' \quad (1)$$

Where P = power dissipation of nanoparticle

$\rho$  = mass density

$\mu_0$  = magnetic permeability of the vacuum [ $4\pi \times 10^{-7} (\text{TmA})^{-1}$ ]

$H_0$  = amplitude of the magnetic field intensity

$\chi''$  = magnetic susceptibility, whose value at working frequency ( $f=170\text{kHz}$ )

The specific absorption rate (SAR) value is significant parameter in the hyperthermia treatment and it is calculated by using,

$$SAR = \frac{\sum_i C_i m_i}{m_{NP}} \left( \frac{dT}{dt} \right) \quad (2)$$

In Eq.2 represents specific heat capacity of the sample, which is the sum of the heat capacity of each constituent  $C_i m_i$  in the magnetic fluid, is divided by the mass of the magnetic nanoparticles  $m_{NP}$  and  $\frac{dT}{dt}$  is the initial slope of the curves.

To hurt the bad cells, the desired heating is achieved using  $\text{NiFe}_2\text{O}_4$  nanoparticles by adjusting the magnetic field and frequency. In terms of the hyperthermia performance of inorganic core with tetramethyl ammoniumhydroxide (TMAH)@ $\text{NiFe}_2\text{O}_4$  nanoparticles, obtained a maximum specific absorption rate (SAR) values between 4 and 11 W/g for field intensities in the range of  $H_0=17.2-23.7\text{kA/m}$  and at frequency  $f = 170\text{kHz}$  from ac-magnetic field induced temperature rise characteristics, where these field parameters are within human tolerable limits, contrary to some studies focusing on hyperthermia applications. The SAR values extracted from the hysteresis region acquired with magnetization measurements are about one order of magnitude higher than the LRT (linear response theory) predicted values, although they are still smaller than the experimental ones. However, due to the non-adiabatic experimental conditions, a bigger region in the dynamic hysteresis curve recorded at the frequency of the hyperthermia experiment ( $f = 170 \text{ kHz}$ ) and a better consistency with the experimental SAR could be expected. In this regard, we can deduce that agglomerated nanoparticles are the primary source of heat generation in the suspension that caused a significant increase in the hyperthermia efficiencies. **Figure 4**, shows the experimental results of such calorimetric measurements performed on the prepared  $\text{NiFe}_2\text{O}_4$  nanoparticle suspension.

**Table 9:** SAR determinants for nickel ferrite nanoparticles

Magnetic compound	Core diameter(nm)	Corona	$H_0$ (KA $\text{m}^{-1}$ )	$\theta$ (Khz)	SAR (W/g)	Ref.
$\text{NiFe}_2\text{O}_4$	$\cong 4.4 \text{ nm}$	tetramethyl ammonium hydroxide	Between 17.2– 23.7	170	11	[44]

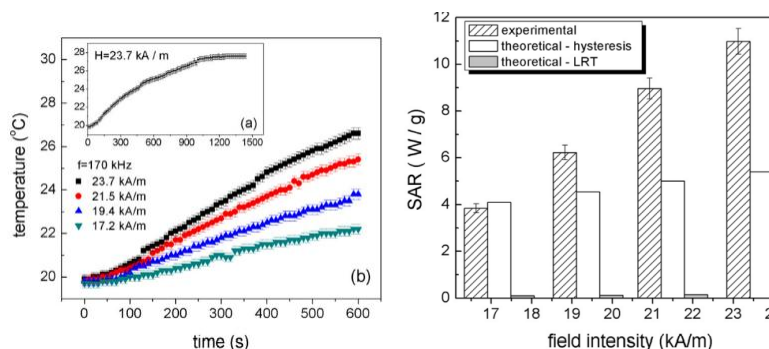


**Figure 4:** AC field-induced temperature rises curves of  $\text{NiFe}_2\text{O}_4$  suspensions in long (inset) and short (main graph) time range, experimentally deduced SAR values in comparison with theoretical values calculated by Eq. (1) and (2)

**Magnetic Resonance Imaging (MRI):** Magnetic resonance imaging is the most important technique in cancer diagnostics which aids to examine the presence, location and size of the tumor. For high saturation magnetization property, chitosan and polyethylene glycol (PEG) are the most studied ones as a coating material in the case of nickel ferrite nanoparticles. With regard to the MRI application of the prepared nanoparticles reported the possible application of chitosan-coated nickel-ferrite ( $\text{NiFe}_2\text{O}_4$ ) nanoparticles as both  $T_1$  and  $T_2$  contrast agents, which depends mainly on the proton density. The coating of nickel-ferrite nanoparticles with chitosan have carried out simultaneously with the synthesis of the nickel-ferrite nanoparticles through chemical co-precipitation method. To demonstrate the  $T_1$  and  $T_2$  effects in an aqueous solution, various concentration samples were prepared and it is determined with an MRI scanner (1.5T MR Scanner, GE Medical Systems). **Figure 5** depicts the plots of  $1/T_1$  and  $1/T_2$  against particle concentration for aqueous solutions of chitosan-coated nickel ferrite nanoparticles[45]. The slopes of the straight lines represent the contrast agent relaxivities. Consequently, the  $T_1$  and  $T_2$  relaxivities ( $r_1$  and  $r_2$ ) were found to be  $0.858 \pm 0.04$  and  $1.71 \pm 0.03 \text{mM}^{-1}$  respectively. The chitosan coated nickel ferrite nanoparticles are suitable as both  $T_1$  and  $T_2$  contrast agents in MRI due to their cylindrical shape, which give rise to both inner and outer sphere processes of nanoparticles. In animal experimentation chitosan coated nanoparticles provide an excellent template for both a 25% signal enhancement in the  $T_1$  weighted image and 71% signal loss in the  $T_2$  weighted image were observed.

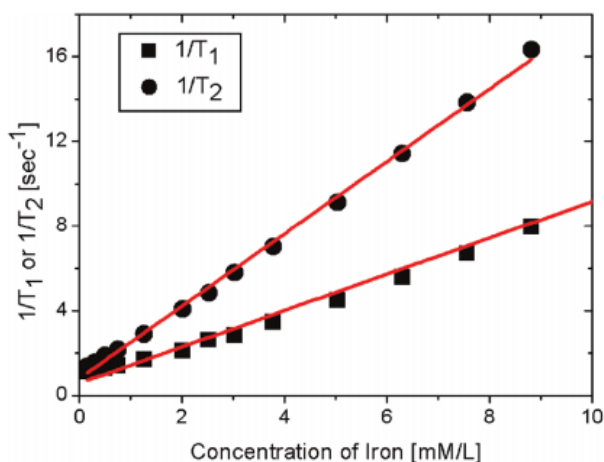


**Figure 5:** Plots of (a)  $1/T_1$  and (b)  $1/T_2$  versus particle concentration for chitosan-coated nickel ferrite nanoparticles

**Table 10:** The longitudinal relaxivity ( $r_1$ ,  $\text{mM}^{-1}\text{s}^{-1}$ ), transverse relaxivity ( $r_2$ ,  $\text{mM}^{-1}\text{s}^{-1}$ ),  $r_2/r_1$  values of polymer coated nanoparticles

Core	Coating	Size (nm)	$r_1(\text{mM}^{-1}\text{s}^{-1})$	$r_2(\text{mM}^{-1}\text{s}^{-1})$	$\frac{r_2}{r_1}$	Ref.
$\text{NiFe}_2\text{O}_4$	PEG	6.1	0.78	36	46	[46]
$\text{NiFe}_2\text{O}_4$	Chitosan	3	0.348	89	256	

### Drug Delivery

Nanotechnology is better suitable for drug targeting of individual tissues and number of advantages over traditional methods. Through the nano-based drug delivery, the transportation of drugs to a specific site provides lowered toxic side effects. The targeted delivery of anticancer drug in and around tumor cells is achieved with an engineered

magnetic nanocarriers. The external localized magnetic field is applied so that it attracts the nanoparticle carrier to the desired site. The surfaces of the nickel ferrite nanoparticles encapsulated with a thick polyethylene glycol (PEG) which is non-magnetic polymer to make them biocompatible and it also escapes from the immune cells[47].

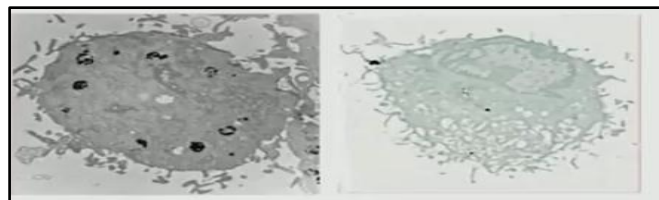


**Figure 6:** Uncoated nickel ferrite nanoparticle enters the phagocyte (immune cells) in very larger amount than the PEG-coated nickel ferrite nanoparticle of similar size and shape.

### Biosensing

Nano-based biosensors can detect things at the even lower concentration. Furthermore, it provides rapid and simple analysis, helps in achieving high sensitivity, specificity, robustness and much more. Due to these properties, it is considered to be a powerful tool to detect at much earlier stage of disease and also the treatment is done prior[48]. Nanomagnetic materials are the significant source which has the unique properties that can be exploited for the development of biosensors. For a specific application, the magnetic nanoparticles are modified in the suitable size, biocompatible linker, chemical composition and magnetic properties of these materials and that permits to use in a variety of instruments and formats for biosensing [49]. Nickel ferrite comes in the category of soft magnetic materials and it has been used in a gas sensor device. It can diagnose, predict and monitor a wide range of diseases from human breath. This can be used for early detection, diagnosis, and staging of cancer can significantly improve human life and impact clinical practice. Obtaining useful information about the early stages of cancer growth can help in the prevention of its growth and metastasis. The tuning ability of MNPs makes them a suitable candidate for diagnostic tools with better sensitivity, easier operation, and systemic sampling. For example, MNPs can remain within the circulatory system and can interact with and collect protein samples of various tissues. The MNPs can later be localized by applying magnetic fields and even retracted for further analysis. MNPs can also be used *in vitro* for continuous monitoring of cell cultures without the need to have a continuous flow system. MNPs can increase the signal strength of absorbed proteins to promote more accurate measurements in turbid samples (such as blood or urine) with no preparation. [48]

**Magnetic separation:** Magnetic separation is the most prevalent technique in biochemical and molecular biological applications that uses magnetism for the isolation, purification and also for the removal of ferromagnetic impurities. This technique has several advantages as compared to other traditional nonmagnetic separation processes. Nickel ferrite nanoparticles possess an excellent magnetic response, thereby they are ideally suitable for the isolation and purification of **histidine-tagged proteins** [50].

The elution was achieved at the imidazole (PEG) concentrations higher than the critical.

## 2. Conclusion

From this paper, it is summed up on the magnetic properties, some important synthesis methods are used to enhance the magnetic properties and the role of nickel ferrite nanoparticles in medical field. Nickel ferrite nanoparticles with great physical and magnetic properties can be produced by various synthesis methods, including conventional and chemical methods which is used for distinct applications. A number of properties such as coercivity, super paramagnetic at room temperature and saturation magnetization make it suitable for hyperthermia is achieved only by proper surface coating. Also, in the current study nickel ferrite nanoparticles are suitable as both  $T_1$  and  $T_2$  contrast agents in MR imaging.

## References

- [1] J. Smit, H.P.J. Wijn. Ferrites, Philips Technical Library: Eindhoven. 1959
- [2] Jaswal, Leena, and Brijesh Singh. "Ferrite materials: A chronological review." *Journal of Integrated Science and Technology* 2, no. 2 (2014): 69-71.
- [3] Stijntjes, Theo, and Bob van Loon. "Early Investigations on Ferrite Magnetic Materials by JL Snoek and Colleagues of the Philips Research Laboratories Eindhoven." *Proceedings of the IEEE* 96, no. 5 (2008): 900-904.
- [4] S. Jie, W. Lixi, X. Naicen, Z. Qito. Microwave electromagnetic and absorbing properties of Dy 3+ doped MnZn ferrites. *J. Rare Earths*. 2010, 28, 451.
- [5] B.D. Giri, J. Nayak, B.B. Shriharsha T., P. Pradhan, N.K. Prasad et.al. Preparation and Cytotoxic Evaluation of Magnetite (Fe<sub>3</sub>O<sub>4</sub>) Nanoparticles on Breast Cancer Cells and its Combinatory Effects with Doxorubicin used in Hyperthermia. *J. Pramana Phys.* 2005, 65, 663.
- [6] R. Valenzuela. magnetic ceramic. Cambridge press, 1994.
- [7] E.S. Murdock, R.F. Simmons. Roadmap for 10 Gbit/in<sup>2</sup> media: challenges. *IEEE Trans. Magnetic*. 1992, 28(5), 3078.
- [8] de Melo Costa, Ana Cristina Figueiredo, Lucianna Gama, M. R. Morelli, and Ruth Herta Goldsmith Aliaga Kiminami. "Nickel ferrite: combustion synthesis, characterization and magnetic properties." In *Materials science forum*, vol. 498, pp. 618-623. Trans Tech Publications Ltd, 2005.
- [9] Ajinka, N.; Yu, X.; Kaithal, P.; Luo, H.; Somani, P.; Ramakrishna, S. Magnetic iron oxide nanoparticle (IONP) synthesis to applications: Present and Future. *Materials* 2020, 13, 4644.
- [10] Dippong, Thomas, Erika Andrea Levei, and Oana Cadar. "Recent Advances in Synthesis and Applications of MFe<sub>2</sub>O<sub>4</sub> (M= Co, Cu, Mn, Ni, Zn) Nanoparticles." *Nanomaterials* 11, no. 6 (2021): 1560.
- [11] Rodrigues, Ana Rita O., I. Tarroso Gomes, Bernardo G. Almeida, João P. Araújo, Elisabete MS Castanheira, and Paulo JG Coutinho. "Magnetic liposomes based on nickel ferrite nanoparticles for biomedical applications." *Physical Chemistry Chemical Physics* 17, no. 27 (2015): 18011-18021.
- [12] Masaru Tada, Takashi Kanemaru, Takeshi Hara, Takashi Nakagawa, Hiroshi Handa and Masanori Abe, *J. Magn. Magn. Mater.* 321 (2009) 1414.
- [13] Dippong, T.; Levei, E.A.; Cadar, O. Formation, structure and magnetic properties of MFe<sub>2</sub>O<sub>4</sub>@SiO<sub>2</sub> (M = Co, Mn, Zn, Ni, Cu) nanocomposites. *Materials* 2021, 14, 1139.
- [14] Mozaffari, M.S.; Amighian, J.; Darsheshdar, J.A.E. Magnetic and structural studies of nickel-substituted cobalt ferrite nanoparticles, synthesized by the sol-gel method. *J. Magn. Magn. Mater.* 2018, 350, 19-22.
- [15] Torkian, S.; Ghasemi, A.; Razavi, R.S. Cation distribution and magnetic analysis of wideband microwave absorptive Co<sub>x</sub>Ni<sub>1-x</sub>Fe<sub>2</sub>O<sub>4</sub> ferrites. *Ceram. Int.* 2017, 43, 6987-6995.
- [16] Ati, A.A.; Othaman, Z.; Samavati, A. Influence of cobalt on structural and magnetic properties of nickel ferrite nanoparticles. *J. Mol. Struct.* 2013, 1052, 177-182.
- [17] Ortiz-Quinñonez, J.-L.; Pal, U.; Villanueva, M.S. Structural, magnetic, and catalytic evaluation of spinel Co, Ni, and Co-Ni ferrite nanoparticles fabricated by low-temperature solution combustion process. *ACS Omega* 2018, 3, 14986-15001.
- [18] Padmapriya, G.; Manikandan, A.; Krishnasamy, V.; Jaganathan, S.K.; Arul Antony, S. Spinel Ni<sub>x</sub>Zn<sub>1-x</sub>Fe<sub>2</sub>O<sub>4</sub> (0.0 ≤ x ≤ 1.0) nano-photocatalysts: Synthesis, characterization and photocatalytic degradation of methylene blue dye. *J. Mol. Struct.* 2016, 1119, 37-39.
- [19] Phumying, S.; Labuayai, S.; Swatsitang, E.; Amornkitbamrung, V.; Maensiri, S. Nanocrystalline spinel ferrite (MFe<sub>2</sub>O<sub>4</sub>, M = Ni, Co, Mn, Mg, Zn) powders prepared by a simple aloe vera plant-extracted solution hydrothermal route. *Mater. Res. Bull.* 2013, 48, 2060-2065.
- [20] Chakradhary, V.K.; Ansaria, A.; Akhtar., M.J. Design, synthesis, and testing of high coercivity cobalt doped nickel ferrite nanoparticles for magnetic applications. *J. Magn. Magn. Mater.* 2019, 469, 674-680.
- [21] Karpova, T.; Vassiliev, V.; Vladimirova, E.; Osotov, V.; Ronkin, M.; Nosov, A. Synthesis of ultradisperse NiFe<sub>2</sub>O<sub>4</sub> spinel by thermal decomposition of citrate precursors and its magnetic properties. *Ceram. Int.* 2012, 38, 373-379.
- [22] Kiran Babu, L.; Rami Reddy, Y.V. A novel thermal decomposition approach for the synthesis and properties of superparamagnetic nanocrystalline NiFe<sub>2</sub>O<sub>4</sub> and its antibacterial, electrocatalytic properties. *J. Supercond. Novel Magn.* 2020, 33, 1013-1021.
- [23] Feng, S.; Yang, W.; Wang, Z. Synthesis of porous NiFe<sub>2</sub>O<sub>4</sub> microparticles and its catalytic properties for methane combustion. *Mater. Sci. Eng. B* 2011, 176, 1509-1512.
- [24] Alarifi, A.; Deraz, N.M.; Shaban, S. Structural, morphological and magnetic properties of NiFe<sub>2</sub>O<sub>4</sub> nano-particles. *J. Alloy Comp.* 2009, 486, 501-506.
- [25] Perron, H., T. Mellier, C. Domain, J. Roques, E. Simoni, R. Drot, and H. Catalette. "Structural investigation and electronic properties of the nickel



- ferrite NiFe<sub>2</sub>O<sub>4</sub>: a periodic density functional theory approach." *Journal of Physics: Condensed Matter* 19, no. 34 (2007): 346219.
- [26] Amiri, S., and H. Shokrollahi. "The role of cobalt ferrite magnetic nanoparticles in medical science." *Materials Science and Engineering: C* 33, no. 1 (2013): 1-8.
- [27] Adam, A., Z. Ali, E. Abdeltwab, and Y. Abbasa. "Magnetic and structural investigations of nanocrystalline nickel ferrite NiFe<sub>2</sub>O<sub>4</sub>." *Journal of Ovonic Research Vol* 5, no. 5 (2009): 157-165.
- [28] Nasheeda P, T Raguram, K S Rajni, "Structural and Magnetic Properties of Nickel Ferrite Nanoparticles Using Citric Acid as Chelating Agent," *Science*, Vol.5, pp. 148-157, June 2018.
- [29] Anjaneyulu, T., A. T. Raghavender, K. Vijaya Kumar, P. Narayana Murthy, and K. Narendra. "Influence of zinc doping in nickel ferrite nanoparticles synthesized by using an oxalic-acid-based precursor method." *Journal of the Korean Physical Society* 62, no. 8 (2013): 1114-1118.
- [30] Chakradhary, Vishal K., Azizurrahman Ansari, and M. Jaleel Akhtar. "Design, synthesis, and testing of high coercivity cobalt doped nickel ferrite nanoparticles for magnetic applications." *Journal of Magnetism and Magnetic Materials* 469 (2019): 674-680.
- [31] Kesavamoorthi, R., and C. Raja. "Studies on the Properties of Manganese Substituted Nickel Ferrite Nanoparticles." *Journal of Superconductivity & Novel Magnetism* 29, no. 11 (2016).
- [32] L. Neel, *Ann. Phys. Paris* 3, 137 (1948).
- [33] Kamala Bharathi, K., and G. Markandeyulu. "Ferroelectric and ferromagnetic properties of Gd substituted nickel ferrite." *Journal of Applied Physics* 103, no. 7 (2008): 07E309.
- [34] Anila I, Subin P. John, Jacob Mathew M. "Synthesis and Characterization of Nickel Ferrite Nanoparticles Prepared by Spray Pyrolysis Method", vol 3, pp. 212-219, November-December-2017.
- [35] Y. Konishi, T. Kawamura, S. Asai, *Ind. Eng. Chem. Res.* 35 (1996), p. 320
- [36] Rio, Irina SR, Ana Rita O. Rodrigues, Carolina P. Rodrigues, Bernardo G. Almeida, A. Pires, A. M. Pereira, J. P. Araújo, Elisabete Castanheira, and Paulo JG Coutinho. "Development of novel magnetoliposomes containing nickel ferrite nanoparticles covered with gold for applications in thermotherapy." *Materials* 13, no. 4 (2020): 815.
- [37] K. Kavitha, T.S. Keerthi, T.T. Mani, *Int. J. Appl. Biol. Pharm. Tech.* 2 (2011) 245-258.
- [38] D.H. Kim, K.N. Kim, K.M. Kim, Y.K. Lee, *J. Biomed. Mater. Res. A* 1 (2009) 1-11.
- [39] N. Kohler, C. Sun, A. Fichtenholtz, *J. Small* 2 (2006) 785-792.
- [40] O. Veiseh, C. Sun, J. Gunn, *J. Nano lett.* 5 (2005) 1003-1008.
- [41] A.K. Gupta, A.S. Cutris, *J. Mater. Sci. Mater. Med.* 15 (2004) 493-496.
- [42] T. Niidome, Y. Akiyama, M. Yamagata, T. Kawano, T. Mori, Y. Niidome, Y. Katayama, *J. Biomater. Sci. Polym. Ed.* 9 (2009) 1203-1215.
- [43] A. Józefczak, T. Hornowski, A. Skumiel, M. Łabowski, M. Timko, P. Kopčanský, J. Magn. Mater. 321 (2009) 1505-1508.
- [44] Umut, Evrim, Mustafa Coşkun, Francesco Pineider, Debora Berti, and Hakan Güngüneş. "Nickel ferrite nanoparticles for simultaneous use in magnetic resonance imaging and magnetic fluid hyperthermia." *Journal of colloid and interface science* 550 (2019): 199-209.
- [45] Ahmad, Tanveer, Hongsub Bae, Yousaf Iqbal, Ilsu Rhee, Sungwook Hong, Yongmin Chang, Jaejun Lee, and Derac Sohn. "Chitosan-coated nickel-ferrite nanoparticles as contrast agents in magnetic resonance imaging." *Journal of Magnetism and Magnetic Materials* 381 (2015): 151-157.
- [46] Banerjee, Abhinandan, Barbara Blasiak, Eva Pasquier, Boguslaw Tomanek, and Simon Trudel. "Synthesis, characterization, and evaluation of PEGylated first-row transition metal ferrite nanoparticles as T 2 contrast agents for high-field MRI." *RSC advances* 7, no. 61 (2017): 38125-38134.
- [47] Phadatar, Manisha R., V. M. Khot, A. B. Salunkhe, N. D. Thorat, and S. H. Pawar. "Studies on polyethylene glycol coating on NiFe<sub>2</sub>O<sub>4</sub> nanoparticles for biomedical applications." *Journal of Magnetism and Magnetic Materials* 324, no. 5 (2012): 770-772.
- [48] Singh, Jay, Appan Roychoudhury, Manish Srivastava, Vidhi Chaudhary, Radha Prasanna, Dong Won Lee, Seung Hee Lee, and B. D. Malhotra. "Highly efficient bienzyme functionalized biocompatible nanostructured nickel ferrite-chitosan nanocomposite platform for biomedical application." *The Journal of Physical Chemistry C* 117, no. 16 (2013): 8491-8502.
- [49] Farzin, Ali, Seyed Alireza Etesami, Jacob Quint, Adnan Memic, and Ali Tamayol. "Magnetic nanoparticles in cancer therapy and diagnosis." *Advanced healthcare materials* 9, no. 9 (2020): 1901058.
- [50] Chun, Jinyoung, Sang Woo Seo, Gyoo Yeol Jung, and Jinwoo Lee. "Easy access to efficient magnetically recyclable separation of histidine-tagged proteins using superparamagnetic nickel ferrite nanoparticle clusters." *Journal of Materials Chemistry* 21, no. 18 (2011): 6713-6717.